Available online at www.sciencedirect.com
ScienceDirect
Cement and Concrete Research 37 (2007) 175–183
Cement and Concrete Research

Alkali–aggregate reaction in activated fly ash systems

I. García-Lodeiro *, A. Palomo *, A. Fernández-Jiménez

Eduardo Torroja Institute (CSIC), Serrano Galvache 4 - 28033 Madrid, Spain

Received 22 November 2005; accepted 2 November 2006

Abstract

Certain aspects of the durability of a new cementitious material, alkali activated fly ash, are addressed in this article; specifically, a series of findings relating to the alkali-silica reaction are reported. The approach adopted in the study was to compare the new cementitious systems to analogous Portland cement mortars using aggregates of differing reactivity and a procedure based on the test described in ASTM standard C 1260. The results of SEM/EDX and XRD analysis of the materials showed that activated fly ash mortars performed better than the Portland cement equivalents.

Keywords: Alkali-activated fly ash; Alkali–aggregate reaction; NBRI test

1. Introduction

Today Portland cement concrete is the construction material *par excellence*. Its cost-effectiveness, mechanical strength and durability have made it indispensable to the construction industry. The exceptionally high temperatures (1400–1500 °C) required, however, make Portland cement production a very costly, energy-intensive process. In addition, large amounts of CO_2, one of the main greenhouse gases, are released into the atmosphere during clinker manufacture. Finally, the durability of traditional Portland cement concrete is limited by a number of factors, most prominently the developments associated with the alkali–aggregate reaction. In light of these problems, the scientific community has undertaken to seek new processes, technologies and materials to provide the construction industry with alternative binders.

The alkali–aggregate reaction is a chemical process involving alkaline oxides generally deriving from the alkalis in the cement and certain forms of reactive silica present in the aggregate. Silex is one of the many types of aggregate that may give rise to the ASR. The mineralogical composition of this compound may vary from opaline to cryptocrystalline silica and from chalcedony to microcrystalline quartz. In alkaline environments, these forms of silica are susceptible to attack, ultimately leading to the dissolution of the aggregate. Such mineralogical forms are, in fact, regarded to be potentially reactive [1–3]. And there is evidence to suggest that a certain concentration or proportion of reactive aggregate, if combined with a given amount of inert aggregate, prompts maximum expansion giving rise to what is known as the concept of the "pessimum" proportion effect [1,4,5].

One measure that has been successfully used to control ASR-induced expansion is the partial replacement of Portland cement with fly ash [6–9]. The role of the ash in curbing expansion is attributed to a number of factors, including the reduced alkalinity in the solution saturating the concrete pores, the lower available calcium content in the system and so on. The presence of calcium has long been controversial and even today the role played by that element in alkali–aggregate reaction mechanisms is poorly understood [10–13].

The present article reports on research focusing on a new binder known as alkali-activated fly ash (AAFA). In mortar and concrete made with such binders, Portland cement can be 100% replaced with fly ash and the mixing water with an alkaline solution [14,15]. Alkali activation of fly ash is a chemical process in which the vitreous component of this industrial by-product is converted into a compact material with cementitious properties. The primary reaction product is a three-dimensional

* Corresponding authors. Tel.: +34 913020440; fax: +34 913026047.
E-mail addresses: iglodeiro@ietcc.csic.es (I. García-Lodeiro), palomo@ietcc.csic.es (A. Palomo).

0008-8846/$ - see front matter © 2006 Elsevier Ltd. All rights reserved.
doi:10.1016/j.cemconres.2006.11.002

Table 1
The granulometry distribution of the aggregate used

Sieve size		
Passing	Retained on	Mass, %
4 mm	2 mm	10
2 mm	1 mm	25
1 mm	500 μm	25
500 μm	250 μm	25
250 μm	125 μm	15

alkaline aluminosilicate gel whose silicon tetrahedra are co-ordinated with aluminium tetrahedra. Crystalline zeolites such as herschelite, hydroxysodalite and so on are obtained as secondary products [16–18].

Alkaline cements and concretes, in general, are characterized by high alkali content but also by low calcium content. As a result of all the foregoing, these materials might be expected to exhibit a different behaviour than Portland cement with respect to the alkali–aggregate reaction.

The purpose of the present study, then, was to evaluate the performance of these new alkaline binders (made with a class F, low calcium content fly ash) in the context of the ASR and compare their behaviour to the findings for traditional Portland cement concrete. The experimental approach involved using aggregates with different degrees of reactivity, among them a "pessimum" proportion aggregate mix.

2. Experimental

2.1. Materials

The materials used in this study were as follows:

- Class F (according to ASTM standard C 618-03) fly ash from a Spanish steam power plant.
- Type I low alkali content Portland cement from a Spanish cement factory.
- Arcosic sandstone with carbonatic cement (Siliceous aggregate) commonly used to manufacture concrete.
- Reactive opal aggregate supplied by CELITE, S.A.

The aggregate was crushed, ground and sieved to the particle size distribution shown in Table 1. Table 2 gives the chemical characteristics of the raw materials used. Ash composition was determined as recommended in Spanish standards UNE 80-125-88 and UNE 80-225-93. Cement and aggregate chemical composition was established with a PHILIPS PW 1404 X-ray fluorescence spectrometer. The prime materials were also characterized for mineralogy and microstructure with a PHILIPS PW 1710-LINK X-ray diffractometer.

Table 3
Mortar features

Mix	(1) SA content (g)	(2) RA content (g)	OPC content (g)	Fly ash content (g)	Activator	(3) L/S ratio
OPC1	1350	0	600	0	–	0.47
OPC2	0	1350	600	0	–	0.47
*OPC3	1215	135	600	0	–	0.47
FA1	1350	0	0	600	Na(OH) 8M	0.47
FA2	0	1350	0	600	Na(OH) 8M	0.47
*FA3	1215	135	0	600	Na(OH) 8M	0.47

(1) Siliceous aggregate; (2) opal aggregate (3) water/cement ratio or solution/ash ratio in fly ash systems. *In OPC 3 and FA3 mortars, the siliceous and opal aggregates were mixed in a proportion of 90:10 by weight to induce the "pessimum" proportion effect [5,19].

2.2. Method

2.2.1. Mortars preparation

The method used to evaluate the possible appearance of the ASR in the specimens was based on ASTM standard C1260-94. This method estimates the deterioration that the ASR may potentially cause in cement mortars in 16 days. The procedure described in the standard was modified slightly in the present study in terms of the aggregate grain size distribution used, (see Table 1), and the temperature, which was 85 °C instead of the recommended 80 °C.

The mortar specimens were made with the aggregates described above. Three series of specimens were prepared. The first series contained 100% siliceous aggregate, the second 100% opal aggregate and the third a siliceous + opal aggregate mix in a proportion of 90:10 by weight to induce the "pessimum" proportion effect.

Prismatic (2.5 × 2.5 × 28.5 cm) specimens were made from the materials to be tested, Portland cement mortars (as a control) and (Portland cement-free) alkali-activated fly ash mortars.

2.2.2. Mortars curing

OPC Mortars: The (deionized) water/cement ratio used in the Portland cement mortars was 0.47 (see Table 3). After an initial curing in a chamber at 21 °C and 99% relative humidity for 24 h, the prisms were de-moulded, immersed in water and stored in sealed containers in an oven at 85 °C for a further 24 h.

Table 2
Chemical composition of the raw materials

	MgO	Al_2O_3	SiO_2	P_2O_5	SO_3	CaO	Fe_2O_3	$Na_2O_e^*$	Insol.	L.O.I.	Total
Fly ash	1.79	26.42	54.42		0.01	3.21	7.01	2..57	0.78	2.19	99.44
Pórtland cement	1.01	3.31	21.5	0.08	2.93	66.2	2.67	0.46		1.44	99.80
Siliceus aggregate	0.93	6.94	48.5	0.06	0.06	21.1	2.58	1.57		17.4	99.62
Opal aggregate	0.98	0.49	84.0	0.03	0.02	6.02	0.44	0.06		8.44	100

*Na_2Oe: weight percentage Na_2O + 0.658 weight percentage K_2O.

AAFA Mortars: An 8 M solution of NaOH was used as the activator to make the fly ash mortar, which was mixed in the same way as the Portland cement. The "solution/ash" ratio was 0.47. After mixing, the specimens (in their respective moulds) were placed in an oven where the mortars were cured for 20 h at 85 °C in high humidity conditions. Finally, they were removed from their moulds.

2.2.3. Accelerated mortar bar method

After their respective curing processes, both the Portland cement and activated fly ash mortar specimens were immersed in a 1 M NaOH solution and stored in sealed containers in an oven at 85 °C. The specimens were routinely measured for length throughout the duration of the test to determine ASR-induced expansion.

Finally, at the ages of 16 and 90 days, the specimens were studied and characterized by SEM/EDX (with a JEOL JSM 5400 microscope fitted with a LINKS-ISIS energy dispersive microanalysis system) and XRD with the PHILIPS diffractometer mentioned above.

3. Results

3.1. XRD characterization of initial materials

XRD analysis (Fig. 1(a)) showed that the siliceous aggregate (SA) consisted primarily of quartz and calcite, together with small quantities of plagioclases and micas. A small amount of dolomite was also observed. The diffractogram for the opal aggregate (RA) showed opal (amorphous silica) to be the prevailing phase. Small amounts of quartz and calcite were likewise detected in this aggregate, see Fig. 1(a).

Unsurprisingly, the XRD analysis of the Portland cement revealed that the majority phase was alite (tricalcium silicate). The other phases normally present in Portland cement were also observed: belite, gypsum and the interstitial phase (aluminates and ferrites) (Fig. 1(b), OPC).

XRD analysis of the fly ash, in turn, showed that it consisted essentially in a vitreous phase, although minority quartz and mullite crystalline phases were also identified, along with small quantities of hematite (Fig. 1(b) FA).

3.2. Determination of mortar prism expansion

Expansion patterns were determined for each and every one of the mortars listed in Table 3. The expansion curves for the cement and activated fly ash mortars with siliceous aggregate (OPC1 and FA1) are given in Fig. 2(a), (b) depicts the results for cement mortars made with opal aggregate (due to the immediate deterioration of the specimens, no data could be obtained for mortar FA2). Lastly, the expansion curves for cement and activated ash mortars made with a mixed siliceous-opal aggregate (90:10 by weight, or "pessimum" proportion) are shown in Fig. 2(c). All the prisms were tested as stipulated in the standard (ASTM C 1260-94).

A comparison of Fig. 2(a), (b), (c) shows that for Portland cement mortar, the greatest expansion was recorded with the "pessimum" proportion aggregate mix, (system OPC3). After only 4 days of immersion in the 1 M NaOH solution at 85 °C, the material had expanded more than the limit allowed in the standard (0.1%). Moreover, even when 100% theoretically non-reactive siliceous aggregate was used (system OPC1); the expansion limit was also exceeded in a short period of time (9 days). After 90 days (see Fig. 2(d)), typical ASR map cracking could be seen across the entire surface of the specimen. This should be interpreted to mean that, contrary to the initial hypothesis, the siliceous aggregate is "moderately" reactive (this was verified by a petrographic analysis of the aggregate conducted in a previous study, when the presence of small amounts of stressed quartz was detected [19]). Finally, when 100% opal aggregate was used (system OPC2), the expansion limit was reached on the 16th day. Initially, expansion in this system appeared later than in system OPC1. However, at the age of 56 days, the specimens were so severely deteriorated that expansion could not be measured (Fig. 2(f)).

When fly ash mortars were prepared with 100% siliceous aggregate (FA1), by contrast, the expansion limit was not exceeded even after 90 days, see Fig. 2(a). Fig. 2(e) shows that in fact the fly ash system specimens were in perfect condition at

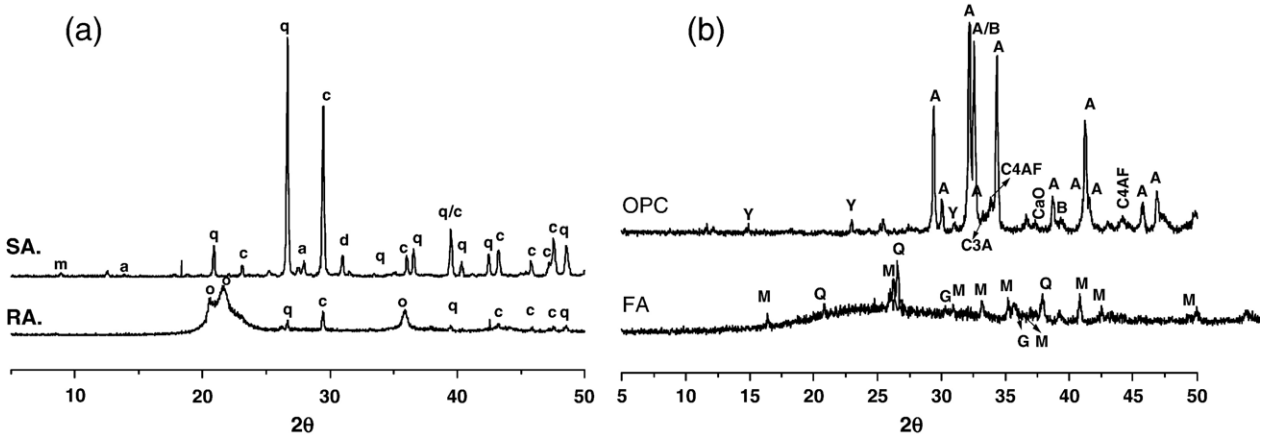

Fig. 1. (a) XRD patterns of siliceous aggregate (SA) and opal aggregate (RA) (b) XRD patterns of Portland cement (OPC) and fly ash (FA); *m* mica *a* plagioclases; *c* calcite; *d* dolomite; *Q* quartz; *o* opal; *Y* gypsum; *A* alite; *B* belite; C_3A tricalcium aluminate; *M* mullite; **G** hematite; C_4AF tetracalcium aluminoferrite; *CaO* lime.

this age, with no surface cracks. When fly ash mortars were prepared with "pessimum" proportion aggregate (FA3), underwent slight expansion, but much more moderately than the respective Portland cement mortars, see Fig. 2(c).

The NaOH-activated fly ash specimens made with 100% opaline aggregate (FA2) were so severely deteriorated after 24 h of immersion in 1 M NaOH that matrix expansion could not be measured. Nonetheless, generally speaking the activated ash systems performed better than the Portland cement systems.

3.3. XRD and SEM/EDX studies of the mortars

The different mortars were studied with XRD and SEM/EDX for mineralogical composition and microstructure after 16 and 90 days of storage in the 1 M NaOH solution at 85 °C. EDX studies were also run at the above ages to determine the elementary composition of the different phases, (see Table 4).

3.3.1. Mortar prepared with 100% siliceous aggregate

Fig. 3(a) shows the diffractograms for OPC1 mortar at 16 and 90 days. According to these results, the aggregate underwent significant change, with a substantial decline in the intensity of the plagioclase signals. The intensity of the portlandite peaks also decreased considerably, which may be interpreted to be a sign of lime uptake by the gel formed in the alkali–silica reaction.

The XRD results for the activated ash systems, in turn, see Fig. 3(b) revealed that they were characterized, among others, by the absence of portlandite and the presence of a series of zeolitic crystalline compounds (herschelite, hydroxysodalite

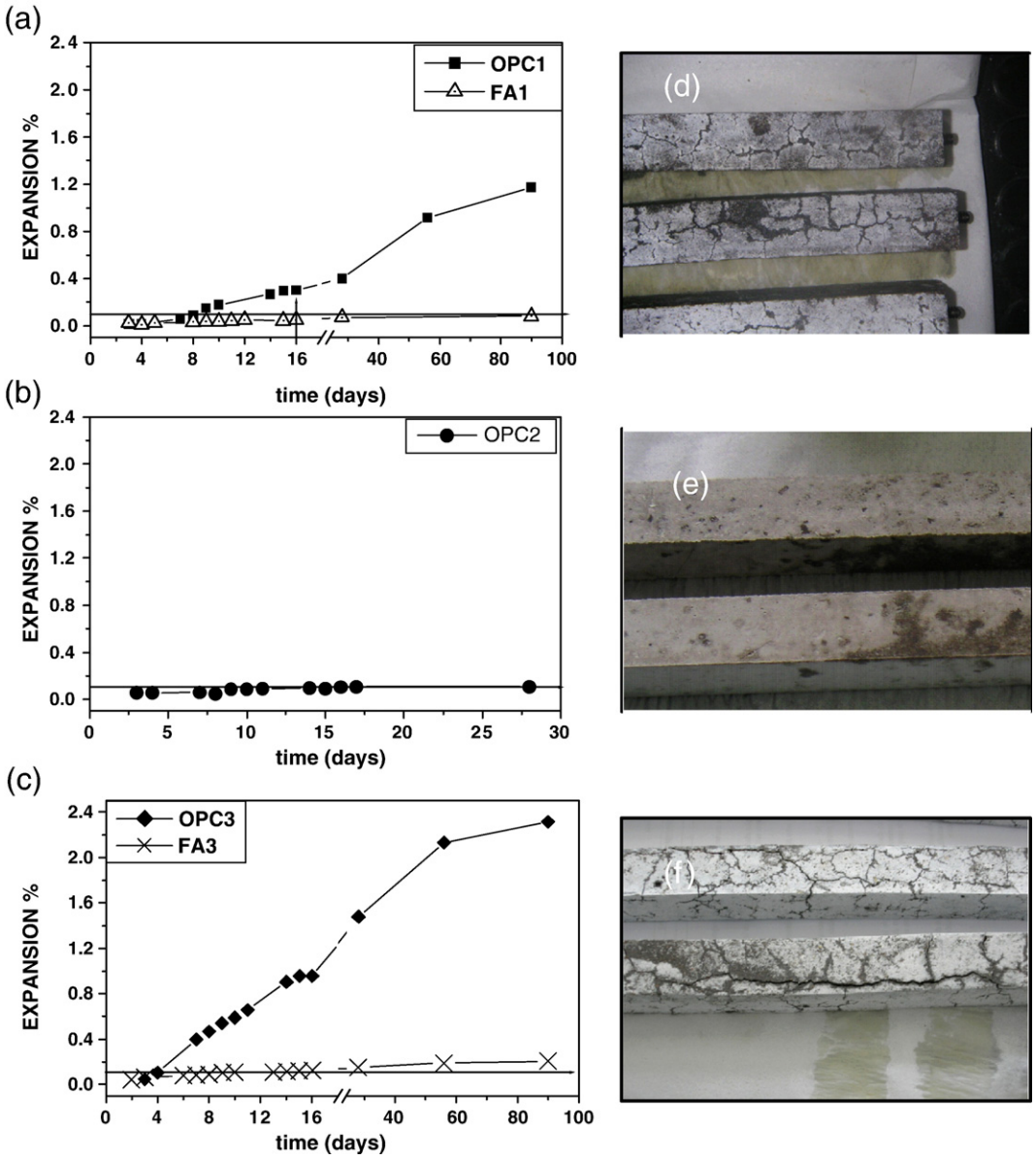

Fig. 2. Expansion curves with the time (a) OPC1 and FA1 mortars (100% of SA) (b) OPC2 mortars (100% of RA); FA2 mortars (No data) (c) OPC3 y FA3 mortars ("pessimum" proportion aggregate). Image of the mortars (d) OPC1 (100% of SA) on the 90th day (e) FA1 (100% of SA) on the 90th day (f) OPC2 (100% of RA) on the 56th day. The features of all mortars are shown in Table 3.

Table 4
Elemental composition determinate by EDX

	Days	P*	Na_2O** (%)	SiO_2** (%)	CaO** (%)	Al_2O_3** (%)	Ca/Si	Na/Si	Si/Al	Na/Al
OPC1	16	1	24.81	28.17	36.05	1.3	1.37	1.70	–	–
		2	2.51	10.59	78.16	–	7.9	0.46	–	–
	90	3	24.67	61.66	10.90	–	0.18	0.77	–	–
FA1	16	4	10.22	45.06	–	39.08	–	–	0.97	0.43
	90	5	15.88	59.62	–	17.67	–	–	2.86	1.47
		6	22.08	63.40	10.20	–	0.17	0.67	–	–
OPC2	16	7	19.89	65.84	12.52	–	0.2	0.58	–	–
OPC3	16	8	32.10	39.68	22.86	–	0.61	1.56	–	–
	90	9	21.10	64.89	11.84	–	0.19	0.63	–	–
FA3	90	10	10.95	62.17	–	17.96	–	–	2.93	1
		11	19.82	65.71	11.93	–	0.19	0.58	–	–

*P**: Analysis number. (1: gel with a high sodium content; 2: portlandite plates; 3: ASR product with a " rod-type" morphology; 4: product of alkaline activation (quasi-amorphous gel) 5: zeolitic crystalline compounds; 6: ASR product with a " rosette/type" morphology; 7: ASR product with a " rosette/type" morphology; 8: ASR product with a " rod-type" morphology; 9: ASR product with a "rosette/type" morphology; 10: zeolitic crystalline compounds 11: ASR product with a "pseudo rosette/type" morphology.
**Content in %.

and zeolite P). Moreover, the intensity of the peaks for these crystalline phases grew with the time of immersion in NaOH at 85 °C while analcime, a new zeolite phase not detected at the age of 16 days, appeared in the 90-day analyses.

At the same time, the 16-day SEM/EDX study of the OPC1 mortars revealed the presence of a gel with a high sodium content in the aggregate–matrix interface, (see Fig. 4(a) and Table 4), point 1), along with portlandite plates (Fig. 4(a) and Table 4, point 2). After 90 days, this same mortar exhibited numerous inward-growing microcracks. A "typical" ASR product was detected in the aggregate–matrix interface with a "rod-type" morphology [20] and Ca/Si and Na/Si ratios of 0.2 and 0.77, respectively, (see Fig. 4(b) and Table 4), point 3.

By contrast, after 16 days of immersion in the 1 M NaOH solution at 85 °C (FA1 mortars), the activated fly ash mortars exhibited only the reaction product typically generated in alkaline activation, see Fig. 5(a), with Si/Al and Na/Al ratios of 0.97 and 0.43, respectively (Table 4, point 4). No calcium was detected in these analyses. The presence of zeolitic crystalline compounds (Fig. 5(b), p.5) was confirmed after 90 days. These crystals, which had high Si/Al and Na/Al ratios (point 5, Table 4), were normally found in gaps in the matrix. Alkali–aggregate reaction products with a pseudo-rosette type morphology and Ca/Si and Na/Si ratios of 0.15 and 0.67, respectively (point 6, Table 4), were also detected, albeit very sporadically.

3.3.2. Mortar prepared with 100% opal aggregate

Fig. 6 gives the X-ray diffraction pattern for OPC2 mortar at the age of 16 days and the pattern of the original opal aggregate. The disappearance of the characteristic peaks for opal (2θ: 22° and 35.8°) in this cement mortar at the age of 16 days provides evidence that reactive silica was attacked and subsequently dissolved. Furthermore, the amount of portlandite in this mortar at the age of 16 days was semi-quantitatively observed to be

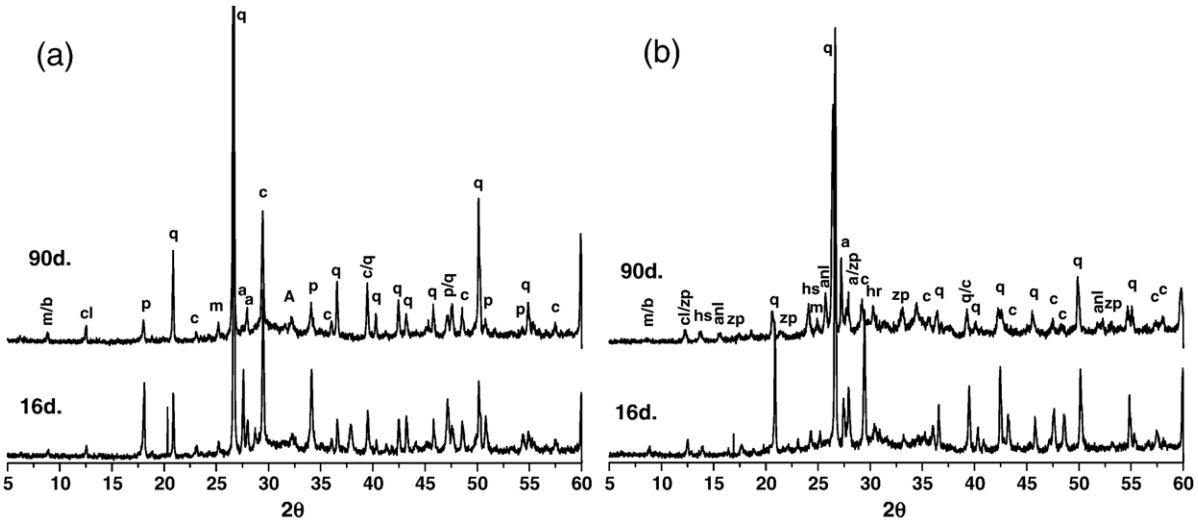

Fig. 3. (a) XRD patterns at 16 and 90 days of OPC1 mortars (b) XRD patterns at 16 and 90 days of FA1 mortars (*q* quartz; *c* calcite; *m* moscovite; *b* biotite; *A* alite; *p* portlandite; *a* plagioclases; *cl* chlorite; *hs* hydroxysodalite; *anl* analcime; *zp* zeolite P; *hr* herschelite).

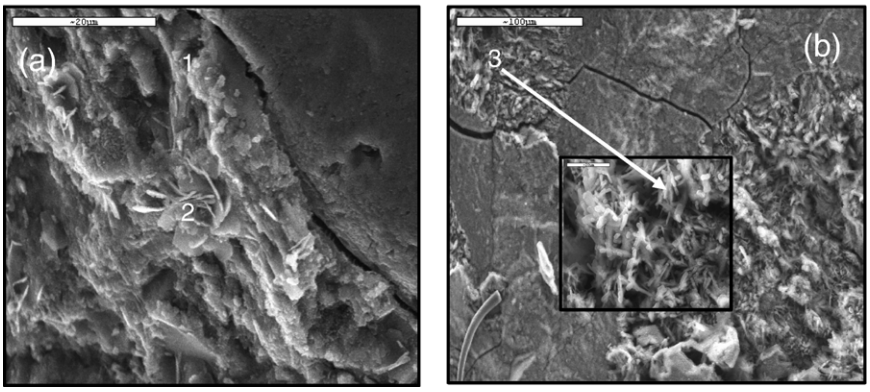

Fig. 4. Photomicrograph of OPC1 mortar (a) At 16 days. (P1) Gel with a high sodium content (P2) Portlandite plates (b) at 90 days. (P3) Cracks in the matrix and ASR product with a "rod-type" morphology.

much smaller than the content in the OPC1 mortar at the same age (see Fig. 3(a)).

The 16-day SEM/EDX analysis clearly revealed the existence of ASR product, here with a rosette-type morphology, (see Fig. 7) previously described in the literature [21]. The Ca/Si and Na/Si ratios for these crystals were 0.2 and 0.58, respectively.

3.3.3. Mortars prepared with the "pessimum" proportion aggregate mix

Fig. 8(a) shows the XRD traces for the OPC3 cement ("pessimum" proportion) mortars. As in the case of OPC1 mortar, the portlandite peaks declined steadily throughout the test, very likely indicating calcium uptake by the gel generated in the alkali–silica reaction. Immersion in 1 M NaOH at 85 °C prompted a decline in plagioclase signal intensity, indicating that the aggregate was under attack. Furthermore, these diffractograms contained no peaks corresponding to opal (reactive silica), which is therefore believed to be attacked very rapidly.

Fig. 8(b) shows the diffractograms for mortar FA3 at 16 and 90 days, in which zeolitic compounds were identified, as in the case of the FA1 mortar. The zeolites present at the age of 16 days were the same as in mortar FA1, but semi-quantitative findings indicated much larger amounts of these crystals in FA3. At this age zeolite P was found to be the predominant crystalline species (with a higher Si/Al ratio than the zeolites observed earlier). This may be explained by the 10% of highly reactive silica in this mortar, which greatly increased the amount of silica available in the initial system. As in the preceding case, analcime was the predominant species at the age of 90 days.

The OPC3 aggregates were observed to be slightly affected in the 16-day SEM/EDX study. Considerable microcracking was detected throughout the matrix, along with an ASR product with rod-type morphology; see Fig. 9 (a), and high silica content (Table 4, point 8). At the age of 90 days, when the expansion limit had been vastly exceeded, see Fig. 2 (c), the specimens were severely cracked and deformed. Large amounts of ASR products with different morphologies (rod and rosette) were detected.

The only species found in 16-day FA3 mortars, in turn, was a typical zeolite precursor generated in alkaline activation, while at 90 days substantial amounts of zeolitic crystalline products were observed, primarily in the gaps in the matrix. Very occasional ASR products with pseudo-rosette morphology (Fig. 9 (c)) were also seen at this age, which might explain the slight expansion detected in these mortars.

4. Discussion

The ASR-induced deterioration of concrete is a serious problem with no simple solution. While there is no lack of traditional methods that attempt to prevent the alkali–silica reaction, such as the choice of appropriately non-reactive

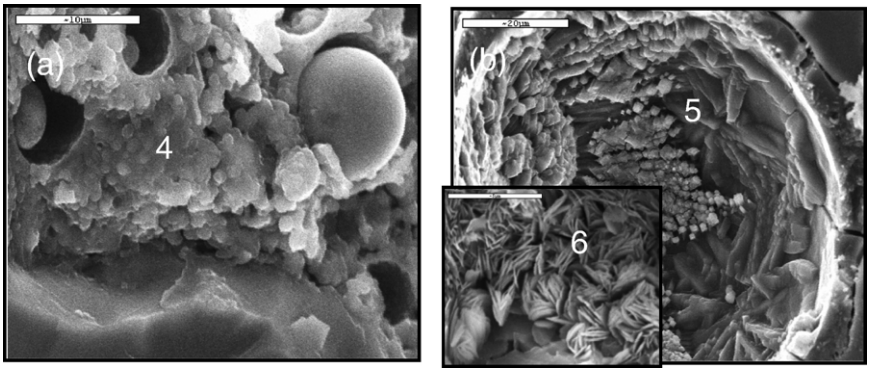

Fig. 5. Photomicrograph of FA1 mortar (a) at 16 days. (P4) product of alkaline activation; (b) At 90 days, zeolitic crystalline compounds in the matrix (P5); ASR product with a "rosette-type" morphology (P6).

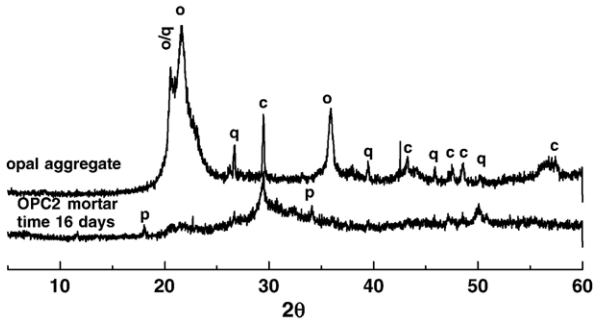

Fig. 6. XRD patterns of opal aggregate and OPC2 mortar at 16 days *Q* Quartz; *o* opal; *p* portlandite; *c* calcite.

aggregate, the use of cementitious materials with a low alkaline content, the addition of pozzolanic materials and so on, the fact is that this problem is increasingly present in Portland cement concrete [22]. Furthermore, repair of the structures affected is a very costly undertaking. In this regard, the research reported hereunder is amply justified.

Perhaps the first feature of this study to merit comment is the "extreme" aggressiveness of the ASTM C1260 test to which the samples were subjected, which caused expansion in the Portland cement systems even when a potentially non-reactive aggregate was used. A previous study found that this aggregate actually contained a certain amount of moderately reactive silica [19]. Despite the intensity of the attack, however, the activated fly ash systems exhibited no significant expansion.

A considerable number of very varied test methods to determine the potential reactivity of aggregates can be found in the extensive literature on the ASR. Berra et al. [23], for instance, conducted a comparative study of different accelerated test methods: chemical tests based on ASTM standard C 289; tests based on XRD analysis and petrographic examination of the aggregate; mortar specimen trials based on the NBRI test (ASTM C 1260) and so on. This last method, which was employed in the present study, affords several advantages: it detects potential aggregate reactivity in a short period of time (16 days) and provides quantitative data on expansion. In short, although fairly aggressive, the test is very useful for the relatively rapid comparison of different systems.

In addition, the interpretation of the results described in this study also entailed an in-depth review of the role of calcium in the formation of expansive ASR products. The role of calcium is the object of a good deal of controversy, although the presence of this element would appear to be fundamental. Several authors [7,8] proved that the addition of $Ca(OH)_2$ promoted ASR-induced expansion and others [13] showed that there is a direct relationship between portlandite uptake and the formation of ASR gels. In the present case, all the conditions required for the formation of expansive products were found in the Portland cement (control) system media. A sufficient supply of alkalis was provided by the NaOH solution, while the chief source of calcium was the portlandite released during cement hydration.

The intensity of the quartz and plagioclase signals in the materials made with Portland cement were found to decline significantly throughout the test, much more acutely in the OPC3 mortars. This is a clear indication that the aggregate was attacked by the alkaline solution in which the mortars were immersed. Similarly, the amount of portlandite present in both systems (OPC1 and OPC3) at the age of 16 days was observed to drop significantly, reaching undetectable levels after 90 days. The calcium in the portlandite was incorporated into ASR-generated expansive gels.

The SEM/EDX study corroborated the formation of alkali–silica reaction products with different morphologies, very similar to the findings described by other authors [20,21]: rod-shaped (typical of gels with high sodium content, normally associated with the early stages of the alkali–silica reaction) and rosette-type crystals (described by Davis and Oberholster [21]). While these crystals had different Ca/Si and Na/Si ratios, the calcium content was fairly high in all (10–12%, (see Table 4)).

The alkali-activated fly ash systems, on the contrary, tended to form a quasi-amorphous gel (Fig. 5 (a)) with high alkali content as the majority reaction product and zeolite crystals such as herschelite, analcime and so on as minority phases, see Fig. 5(b). Since zeolites normally "precipitate" into pre-existing pores in the matrix, their growth generates no stress that might lead to microcracking.

As in the case of the cement systems, the waning intensity of the X-ray diffraction peaks for the various crystalline phases present in FA1 and FA3 mortars provided evidence that the aggregates were under attack. But new zeolite crystalline phases were also found to appear with time.

SEM/EDX analysis of the composition of the phases comprising the FA1 and FA3 mortars tested as described in ASTM standard C 1260 showed that, unlike the products generated by Portland cement hydration, they had a very low calcium content. All the foregoing is believed to be largely responsible for attenuating and retarding the expansion in such systems see Fig. 2(a), (c).

In fly ash-based systems, then, the alkalis were found to be able to interact in two competitive reactions: in the first, they are taken up to activate the vitreous component of the initial ash and convert it into a cementitious material or even form zeolite crystals; but at the same time they may be involved in a second reaction that attacks the aggregate. In the fly ash systems studied here, the primary reaction was clearly alkali activation that led to the formation of an inorganic polymer and a few zeolitic crystalline phases from the vitreous component of the original

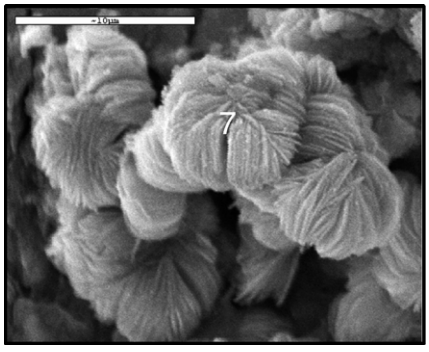

Fig. 7. Photomicrograph of OPC2 mortar at 16 days. ASR product with a "rosette-type" morphology.

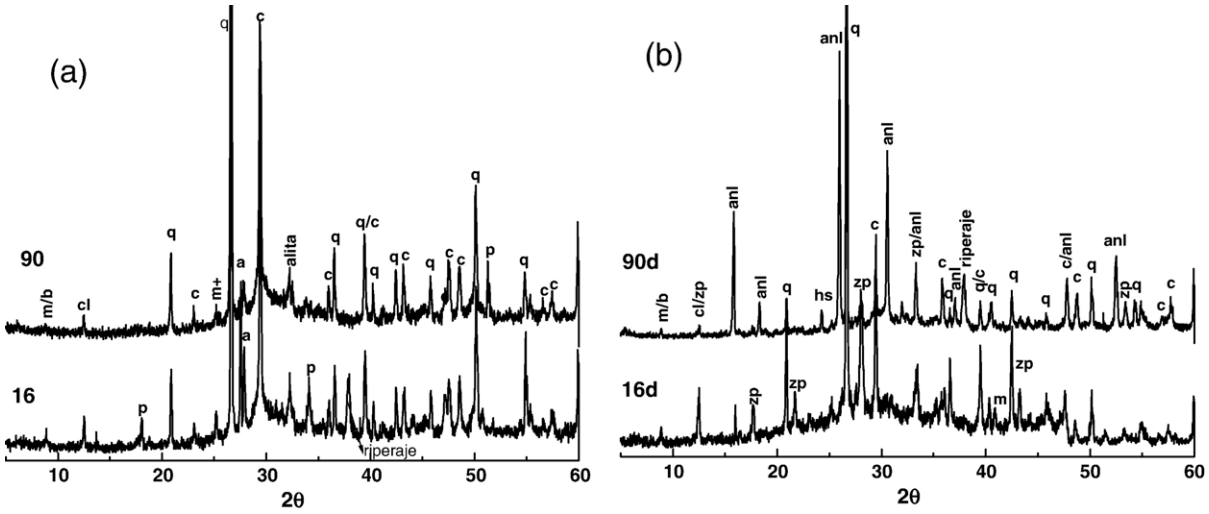

Fig. 8. (a) XRD patterns of OPC3 mortar at 16 and 90 days. (b) XRD patterns of FA3 mortar at 16 and 90 days. (*q* quartz; *c* calcite *m*; moscovite; *b* biotite; *A* alite; *p* portlandite; *a* plagioclases; *cl* chlorite; *hs* hydroxysodalite; *anl* analcime; *zp* zeolite P; *hr* herschelite).

ash with respect the alkali–aggregate reaction it also runs along the time. Fig. 8 is an evidence of how quartz from aggregate is dissolved with time. However due to lack of calcium in these systems, the AAR product is not expansive. Consequently, all the ash systems tested expanded less than the corresponding Portland cement systems, (see Fig. 2). Indeed, only system FA3 exceeded the 0.1% expansion limit, and only after 90 days. Three months in such an aggressive medium may suffice for all the ash to have reacted, leaving the aggregate with no "protection" against the alkaline environment. But even then, since the amount of calcium in the ash systems is minimal, only tiny volumes of expansive ASR gels are formed.

Furthermore, Fig. 8(b) shows that in this case, after 90 days many zeolitic crystalline compounds are formed, with the zeolite analcime ultimately predominating. Such harsh system conditions (with specimens immersed in NaOH for 90 days at 85 °C) induce the formation of zeolitic compounds. Given that some of these, such as analcime, are icositetrahedral crystals that can grow to a very large size inside the matrix, the possible generation of internal stresses by the crystals themselves cannot be ruled out. But this only occurs when the conditions are as aggressive as those tested here. Under real life circumstances the inorganic polymer crystallizes into zeolite very slowly and as these minerals are usually found in gaps in the matrix, the existence of stress that might generate cracking is unlikely.

Finally, another finding that reveals the differences in reactivity between the two cementitious systems in the face of an alkaline attack is the complete destruction of FA2 mortar specimens (ash + 100% opal aggregate) when subjected to the ASTM standard C 1260 test. The key issue to be considered here is that the ash (essentially vitreous silica) was mixed with a large amount of opal, a highly reactive aggregate. The conditions prevailing in the system were therefore already very extreme when the specimens were immersed in 1 M soda at a temperature of 85 °C. Inasmuch as these mortars consisted practically entirely of reactive silica, they were attacked in the alkaline medium.

5. Conclusions

The primary conclusion to be drawn from this study is that cementitious systems based on activated fly ash are less susceptible to generate expansion by alkali–silica reaction than

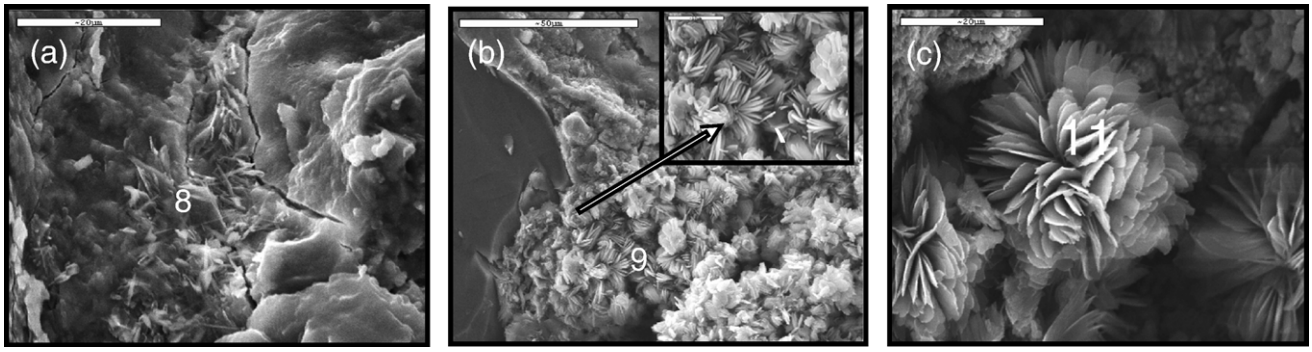

Fig. 9. Photomicrograph of OPC3 mortar (a) At 16 days. ASR product with a "rod-type" morphology (b) at 90 days. Matrix aggregate interface. ASR product. Photomicrograph of FA3 mortar (c) at 90 days. ASR product with a "pseudo rosette-type" morphology.

traditional Portland cement systems. The evidence indicates that the calcium in the materials plays an essential role in the expansive nature of the gels.

In another vein, while the test method used is an aggressive procedure in which mortars are subjected to exceptionally harsh conditions, it provides for very useful inter-system comparisons.

Acknowledgements

The present research was funded by the Ministry of Education and Science through project BIA2004-04835 and by the Spanish Council for Scientific Research in the form of the award of a post-doctoral contract (ref. 13P-PC2004L) to Dr. Ana Fernández-Jiménez. The authors wish also to thank the CSIC and European Social Fund for co-financing pre-doctoral scholarship I3P to Inés García-Lodeiro. Finally to José Luis García and Alfredo Gil for their assistance in this study.

References

[1] R.N. Swamy, in: R.N. (Ed.), The Alkali–Silica Reaction in Concrete, Blackie, New York, 1992.
[2] J. Soriano, M^{a}.A. Bustillo, Influencia de los minerales opalinos en la durabilidad del hormigón. VI Reunión Científica de la Sociedad Española de Mineralogía, Boletín de la Sociedad Española de Mineralogía, Zaragoza (España), 1986, pp. 403–409.
[3] M^{a}.A. Bustillo, J. Soriano, "Contribución al estudio de la reacción álcali-árido" Parte I. Reconocimiento y caracterización de ópalos" Ed. Centro de estudios y Experimentación de Obras Públicas (MOPU), Madrid (España) (1982).
[4] M.A. Ozol, The pessimum proportion as a reference point in modulating alkali–silica reaction, Proceedings of a Symposium on Alkali–Aggregate Reaction, Preventive Measures, Reykjavik (Iceland), 1975, pp. 113–130.
[5] R.J. Collins, Alkali aggregate reactivity in dense concretes containing synthetic or porous natural aggregate, Cem. Concr. Res. 19 (1989) 278–288.
[6] F. Bektas, L. Turanli, T. Topal, Mc Goncuoglu, Alkali reactivity of mortars containing chert and incorporating moderate calcium fly-ash, Cem. Concr. Res. 34 (2004) 2209–2214.
[7] R.F. Bleszynskisnd, Michael D.A. Thomas, Microstructural studies of alkali–silica reaction in Fly-ash Concrete immersed in alkaline solutions, Adv. Cem. Based Mater. 7 (1998) 766–778.
[8] M.H. Shehata, M.D.A. Thomas, The effect of fly ash composition on the expansion of concrete due to alkali–silica reaction, Cem. Concr. Res. 30 (2000) 1063–1072.
[9] M.H. Shehata, M.D.A. Thomas, Use of ternary blends containing silica fume and fly ash to suppress expansion due to alkali silica reaction in concrete, Cem. Concr. Res. 32 (2002) 341–349.
[10] L.S. Dent Glasser, Kataoka, The role of calcium in the alkali–aggregate reaction, Cem. Concr. Res. 12 (1982) 321–331.
[11] S. Chatlerji, The role of $Ca(OH)_2$ in the breakdown of Portland cement concrete due to alkali–silica reaction, Cem. Concr. Res. 9 (1979) 185–188.
[12] M.D.A. Thomas, The role of calcium in alkali–silica reaction, Materials Science of Concrete (Sidney Diamond Symposium), 1998, pp. 325–337, Sidney (Australia).
[13] Xiaoqiang Hou, L.J. Stuble, R. James Kirkpatrick, Formation of ASR gel and the role of CSH and portlandite, Cem. Concr. Res. 34 (2004) 1683–1696.
[14] A. Palomo, A. Férnandez-Jiménez, C. López-Hombrados, J.L. Lleyda, Precast Elements Made of Alkali-Activated Fly Ash Concrete, Eighth CANMET/ACI International Conference on Flyash, Silica Fume, Slag and Natural Pozzolans in Concrete, 2004, Las Vegas, U.S.A.
[15] A. Fernández-Jiménez, A. Palomo, C. López-Hombrados, Engineering properties of alkali activates fly ash concrete, ACI Mater. J. (March–April 2006) 106–112.
[16] A. Fernández-Jiménez, A. Palomo, M. Criado, Microstructure development of alkali-activated fly ash cement: a descriptive model, Cem. Concr. Res. 35 (2005) 1204–1209.
[17] A. Palomo, S. Alonso, A. Fernández-Jiménez, I. Sobrados, J. Sanz, Alkaline activation of fly ashes. A NMR study of the reaction products, J. Am. Ceram. Soc. 87 (2004) 1141–1145.
[18] A. Fernández-Jiménez, A. Palomo, Mid-Infrared spectroscopic studies of alkali-activated fly ash structure, Microporous Mesoporous Mater. 86 (2005) 207–214.
[19] I. García-Lodeiro, A. Palomo, A. Fernández-Jiménez, Alkali–aggregate reaction in alkali-activated fly ash concrete (part II), RILEM Conference on Concrete and Reinforced Concrete, Moscow, 2005, pp. 452–462.
[20] A. Fernández-Jiménez, F. Puertas, The alkali–silica reaction in alkali-activated granulated slag mortars with reactive aggregate, Cem. Concr. Res. 32 (2002) 1019–1024.
[21] G. Davies, R.E. Oberholster, Alkali–silica reaction products and their development, Cem. Concr. Res. 18 (1998) 621–635.
[22] B. Mather, How to make concrete that will not suffer deleterious alkali–silica reaction, Cem. Concr. Res. 29 (1999) 1277–1280.
[23] M. Berra, T. Mangialardi, A.E. Paolini, R. Turriziani, Critical evaluation of accelerated test methods for detecting the alkali-reactivity of aggregates, Adv. Cem. Res. 4 (1991/92) 29–37.